Thin Solid Films 587 (2015) 112–116

Contents lists available at ScienceDirect

Thin Solid Films

journal homepage: www.elsevier.com/locate/tsf

Structural properties of In_2Se_3 precursor layers deposited by spray pyrolysis and physical vapor deposition for $CuInSe_2$ thin-film solar cell applications

P. Reyes-Figueroa [a,b], T. Painchaud [b], T. Lepetit [b], S. Harel [b], L. Arzel [b], Junsin Yi [c,*], N. Barreau [b], S. Velumani [a,c,*]

[a] Department of Electrical Engineering (SEES), Cinvestav-Zacatenco, 2508 Av. IPN, 07360 Mexico City, Mexico
[b] IMN, UMR 6502, Université de Nantes, 2 rue de la Houssinière, 44322 Nantes Cedex 3, France
[c] School of Information and Communication Engineering, 2066 Seobu-ro, Jangan-gu, 440-746 Suwon, Republic of Korea

ARTICLE INFO

Available online 28 January 2015

Keywords:
Indium selenide
Copper indium selenide
Spray pyrolysis
Physical vapor deposition

ABSTRACT

The structural properties of In_2Se_3 precursor thin films grown by chemical spray pyrolysis (CSP) and physical vapor deposition (PVD) methods were compared. This is to investigate the feasibility to substitute PVD process of $CuInSe_2$ (CISe) films by CSP films as precursor layer, thus decreasing the production cost by increasing material-utilization efficiency. Both films of 1 μm thickness were deposited at the same substrate temperature of 380 °C. X-ray diffraction and Raman spectra confirm the formation of γ-In_2Se_3 crystalline phase for both films. The PVD and CSP films exhibited (110) and (006) preferred orientations, respectively. The PVD films showed a smaller full width at half maximum value (0.09°) compared with CSP layers (0.1°). Films with the same crystalline phase but with different orientations are normally used in the preparation of high quality CISe films by 3-stage process. Scanning electron microscope cross-section images showed an important difference in grain size with well-defined larger grains of size 1–2 μm in the PVD films as compared to CSP layers (600 nm). Another important characteristic that differentiates the two precursor films is the oxygen contamination. X-ray photoelectron spectroscopy showed the presence of oxygen in CSP films. The oxygen atoms could be bonded to indium by replacing Se vacancies, which are formed during CSP deposition. Taking account of the obtained results, such CSP films can be used as precursor layer in a PVD process in order to produce CISe absorber films.

1. Introduction

$CuInSe_2$ (CISe) and $Cu(In,Ga)Se_2$ (CIGSe) materials are widely investigated as absorber layers in thin film solar cells. This is mainly due to their high absorption coefficient (10^{-5} cm^{-1}), suitable direct band gap (~1–1.7 eV) and potential low-cost production [1]. Furthermore, CISe and CIGSe solar cells exhibit very good outdoor stability and radiation hardness [2]. In particular, CIGSe thin film solar cells have achieved efficiencies of 20.8% [3]. This efficiency surpasses the best achieved results of multicrystalline silicon and CdTe solar cells [4]. $Cu(In,Ga)Se_2$ films can be deposited by vacuum and non-vacuum methods such as physical vapor deposition (PVD) (e.g. co-evaporation) [5,6], selenization of metal precursor films [7], electrodeposition [8], particulate process (e.g. spin coating, doctor blade) [9–12], and chemical spray pyrolysis (CSP) [13–16].

Non-vacuum deposition methods of CISe have shown significantly lower capital expenditure, reduced material cost and produce devices with considerable efficiencies [14,17,18]. Amongst these methods, the chemical spray pyrolysis deposition has the advantages of low cost equipment, easy scale-up, simple atomization process and temperature control. This deposition is based on the pyrolytic decomposition of small droplets of chloride-based solution sprayed onto a heated substrate under atmospheric conditions [19]. The PVD by co-evaporation method gives the best solar cell efficiencies but poses cost and technological barriers. In this technique, vapors of two different materials are generated simultaneously. These two vapors condense together to form an alloy or a compound. Amongst the different co-evaporation processes, the so-called "3-stage" is essential in obtaining high quality CISe films [20]. This process basically consists of Stage-1: growth of a 1 μm thick In_2Se_3 thin film at low temperature (300–400 °C), Stage-2: these layers are used as precursor during the co-evaporation of copper and selenium, where a Cu-rich film is yielded, Stage-3: indium and selenium are co-evaporated and the film evolves gradually to Cu-poor until the final composition is reached [21]. The In_2Se_3 precursor films used in this process are very important because of i) their direct relationship with the final CISe/CIGSe absorber material quality [22] and ii) its deposition represents around 50% of the total deposition material in a standard 3-stage process [6]. The In_2Se_3 is a III_2–VI_3 semiconductor

* Corresponding authors at: Department of Electrical Engineering (SEES), Cinvestav-Zacatenco, 2508 Av. IPN, 07360 Mexico City, Mexico. Tel.: +52 55 57 47 38 00x2036.
E-mail addresses: yi@skku.ac.kr (J. Yi), velu@cinvestav.mx (S. Velumani).

http://dx.doi.org/10.1016/j.tsf.2015.01.035
0040-6090/

compound that exhibits several phases and crystalline structures (e.g. defected hexagonal, cubic) depending on the deposition conditions.

In this research work, we investigated the feasibility of obtaining CISe films by PVD (e.g. co-evaporation 3-stage) using CSP film as precursor layer by focusing on the structural properties of the In_2Se_3 precursor films obtained from CSP and PVD. This approach could lead to decreased CISe film production cost by increasing the material-utilization efficiency.

2. Experimental details

2.1. Deposition of In_2Se_3 thin films

In_2Se_3 thin films were deposited by PVD and CSP in order to study the difference in the structural properties of the films. A standard 3-stage co-evaporation process uses 1 μm thick In_2Se_3 precursor films deposited at 300–400 °C in order to obtain high quality CISe absorbers [6,22]. For this reason, both PVD and CSP In_2Se_3 layers used in this work were deposited at 380 °C with 1 μm thickness.

2.1.1. Chemical spray pyrolysis process

The In_2Se_3 layers were deposited by CSP on molybdenum coated soda lime glass (SLG) substrates. The CSP films were grown on a molten tin bath at 380 °C. The substrate temperature was monitored by a thermocouple located at the backside of the glass substrate. The details of the CSP setup are described elsewhere [16]. The precursor solutions contain concentrations of 0.0015 M for $InCl_3$ and 0.0055 M for N-N-dimethyl-selenourea (DMSeU) in a 20% volume ethanol aqueous solution. DMSeU was provided in excess of stoichiometry due to the volatile nature of Se at the deposition temperature. The desired pH (4–5) of the solution was achieved by addition of HCl. The total volume of the solution sprayed was 800 ml with a spray rate of 6.5 ml/min with nitrogen as a carrier gas whose flow rate was 1.5 l/min. These parameters yield films of about 1 μm thickness.

2.1.2. Physical vapor deposition process

The In_2Se_3 films of 1 μm thickness were deposited onto Mo/SLG substrates. The elemental fluxes of In and Se were controlled by changing the temperatures of the evaporation sources. A quartz oscillator was used in order to control the evaporation rates and thickness of the film. During the deposition, the substrates were heated by an infrared source. The temperature was monitored by a thermocouple located at the backside of the substrate. The deposition were carried out at a substrate temperature of 380 °C under high vacuum (1×10^{-4} Pa). An effusion cell evaporation source for In and pyrex crucible for Se were used. During the evaporation process, the temperature of In and Se sources were kept at 1010 °C and 285 °C, respectively.

2.2. Thin film characterization

The morphology of the films was observed by scanning electron microscope (SEM)-model JEOL 7600F using an acceleration voltage of 5 kV with a magnification of ×20,000. The average composition of the films was measured by electron dispersive spectroscopy (EDS) using a SEM equipped with an energy dispersive spectrometer SDD SAMx with a resolution of 129 eV, employing a beam current of 0.3 nA and an acceleration voltage of 20 kV. The crystalline quality and orientation were characterized by X-ray diffraction (XRD) using a Cu-Kα radiation (1.541 Å) with a θ/2θ configuration and stepsize of 0.01°. Raman measurements were performed with a Jobin–Yvon T64000 using an argon laser (λ = 514.5 nm) with a probe area around 1 μm^2 for an acquisition time of 5 min. The surface analyses were performed by X-ray photoemission spectroscopy (XPS) in a Kratos Axis Nova with a monochromatic Al K radiation (1486.6 eV) and 160 eV pass energy with an energy step of 0.5 eV. The sputtering was performed for 60 s with an Ar ion beam and beam energy of 300 eV. The C1s signal from adventitious carbon with a binding energy $E_B = 284.6$ eV was used for energy referencing. The peak fit analysis was performed using the CasaXPS software where a linear background was subtracted from the spectra. The spectra were fitted by peaks with a Gauss (60%)–Lorentz (40%) profiles.

3. Results and discussion

3.1. In_2Se_3 thin films grown by PVD

The PVD films were studied by XRD in order to determine their crystalline properties. Fig. 1 shows the diffractogram of PVD-In_2Se_3 thin film grown on Mo/SLG. The films exhibited diffraction peaks corresponding to polycrystalline γ-In_2Se_3. The films have shown (110) orientation with strong (300) and weak (006) lines. This result is in good agreement with the XRD pattern of γ-In_2Se_3 (JCPDS 40-1407) with hexagonal structure [23]. Peaks around 38° and 48° are related to β-In_2Se_3 phase. The peak around 19° does not match with InSe or β-In_2Se_3 phases. The full width half maximum (FWHM) of the (110), (006) and (300) peaks were 0.07, 0.09 and 0.10°, respectively.

The Raman spectrum of the PVD film is shown in Fig. 2a. The main mode located at 149.4 cm^{-1} is related to the formation of a stable polycrystalline γ-In_2Se_3 phase [24]. The Raman modes located around 178 and 203 cm^{-1} are related to both γ-In_2Se_3 [24] and α-In_2Se_3 [25]. The vibrational modes located at around 149 and 227 cm^{-1} appear at the same wave number reported by Wanatabe and Marsilliac et al. [26,27]. This result is consistent with the XRD diffraction measurements.

The surface morphology and cross-section SEM images of PVD In_2Se_3 films are shown in Fig. 3a,b. Surface morphology shows lamellar structures with different grain sizes and also hexagonal grains with 1–2 μm width. These hexagonal grains are related to the growth of the films with (001) orientation. The cross-section image (Fig. 3a) exhibited densely packed columnar structure (~0.8–1 μm). The observed morphologies were attributed to the high surface mobility of adatoms impinging on the surface of the substrate during nucleation stage. The relative chemical composition of the PVD-In_2Se_3 film without considering the oxygen content is shown in Table 1.

The surface of the PVD-In_2Se_3 films was studied by XPS. Fig. 4 shows the O1s core level spectra recorded from un-clean and ion sputtered surface of PVD films. The O1s peak obtained from un-clean surface

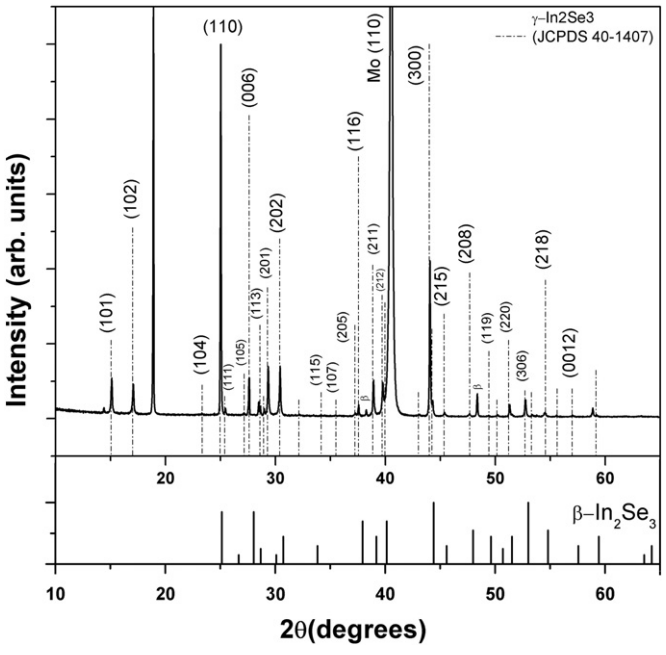

Fig. 1. XRD pattern of the In_2Se_3 film grown by PVD.

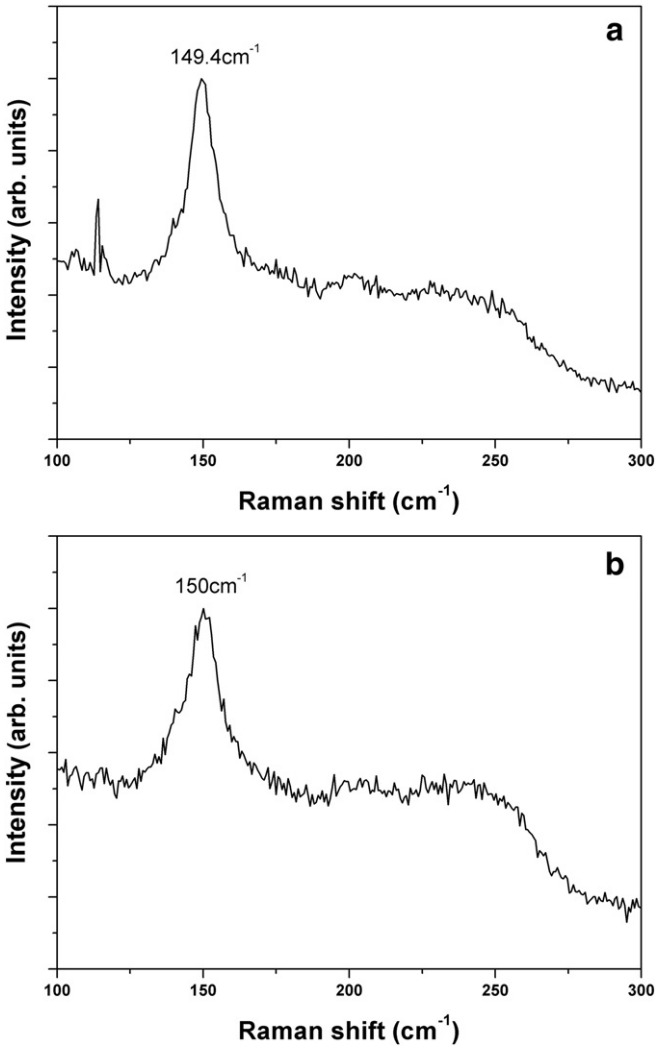

Fig. 2. Raman spectroscopy of the In_2Se_3 film grown by PVD (a) and CSP (b) techniques.

could be separated into at least two sub-bands located at 531.28 and 529.76 eV. The peak at higher binding energy (BE) is characteristic of surface contaminated by oxygen from air. The peak at lower BE could be corresponding to the oxygen bonded to a metal [28]. After ion sputtering almost all the O1s peak signal is lost and the remaining peak is situated at 529.9 eV, corresponding to a portion of oxygen content still bonded to the metal.

3.2. In_2Se_3 thin films grown by CSP

Fig. 5 shows the XRD of the CSP-In_2Se_3 thin film grown on Mo/SLG. Similar to PVD films, the CSP film exhibited diffraction peaks related to polycrystalline γ-In_2Se_3 phase. This is in good agreement with the XRD pattern of γ-In_2Se_3 (JCPDS 40-1407) with hexagonal structure [23]. Contrary to the (110)-oriented PVD films, the CSP film exhibited (006) orientation with weak (110) and (300) lines. In results reported by Mise et al. [22] it is observed that Cu(In,Ga)Se_2 films with same (112) orientation are obtained by using a (110) or (006)-oriented In_2Se_3 precursor films. It is known that during the CSP deposition, the substrate temperature of the front surface is lower (15–20 °C) than the back of the substrate where the thermocouple is located [29]. This decrease is due to the difference in temperature of the sprayed precursor solution (15–25 °C) and the substrate temperature (380 °C). Thus, the substrate temperature during CSP deposition is lower than 380 °C. Thus, one reason for the change in orientation could be the lower growth temperature used in the CSP deposition as compared to the PVD. Mise et al. [22] have reported a similar behavior of $(In,Ga)_2Se_3$ films. The difference in temperature is also present in the CVD process but, given that the precursor materials reaching the substrate are evaporated at relative high temperatures (1010 °C and 285 °C), the difference is less than in CSP deposition. Another reason for the (006)-dominant peak obtained by CSP film could be the formation of a Se-deficient In_2Se_3 phase. The chemical composition of the CSP-In_2Se_3 layer is shown in Table 1. The composition of both PVD and CSP films is slightly different. The Se/In ratio is observed to be lower in the CSP deposited films. This could be related to the re-evaporation of Se from the hot substrate in the open-air atmosphere. Thus, it is possible to assume the formation of more Se vacancies in the CSP films. These results are in good agreement

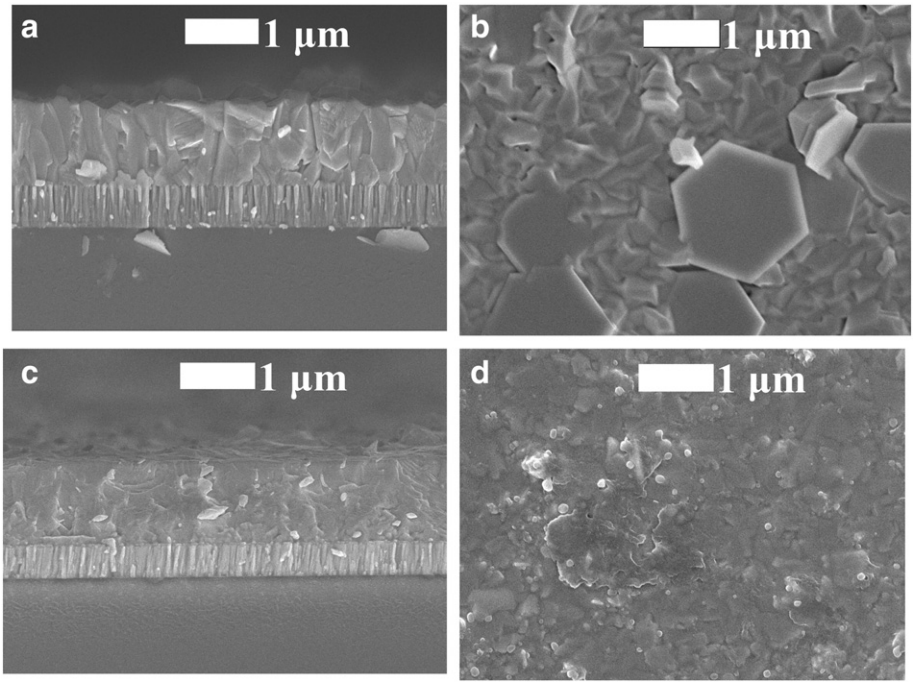

Fig. 3. SEM images of the In_2Se_3 film grown by PVD (a,b) and CSP (c,d) techniques.

Table 1
Composition analysis of PVD and CSP In_2Se_3 thin films and the respective Se/In relative ratio without considering the oxygen content.

Sample	In (at.%)	Se (at.%)	Se/In
PVD-In_2Se_3	42.91 (±1.08)	57.08 (±0.66)	1.33
CSP-In_2Se_3	44.44 (±1.28)	55.57 (±0.56)	1.25

with the XRD, SEM and Raman spectroscopy of γ-In_2Se_3 films with a (006)-dominant peak. A similar trend has been reported by Ishizuka et al. [30]. There is no clear evidence of β-In_2Se_3 phase or oxide (e.g. In_2O_3) formation. The FWHM of (110), (006) and (300) peaks were 0.09, 0.10 and 0.15°, respectively. The smaller FWHM value of PVD in relation to CSP layers corresponds to a better crystalline quality of the former.

The γ-In_2Se_3 structure was also identified by Raman spectra (Fig. 2b). The strong vibrational modes located around 150 and 227 cm^{-1} are related to γ-In_2Se_3 phase [24]. The Raman mode located around 203 cm^{-1} is related to both γ-In_2Se_3 [24] and β-In_2Se_3 [25]. It is possible to observe that the Raman spectra of PVD and CSP films have the same vibrational modes related to γ-In_2Se_3 phase, indicating the similarity in their structure. The structure of the In2Se3, which belongs to the $A_2^{III}B_3^{VI}$ series of compounds based on tetrahedral atomic coordination with one third of the cation sites empty. The observed vibrational modes are related to the γ-In_2Se_3 phase distorted wurtzite-like structure in which half of In atoms are tetrahedrally coordinated and the remaining half are pentagonally coordinated in a bipyramid form and the Se atoms are three-fold coordinated [23].

Fig. 3c,d shows the SEM images of the CSP-In_2Se_3 films deposited on Mo/SLG. Fig. 3d shows a granular surface morphology with different grain sizes (60–600 nm). This morphology is related to the growth of In_2Se_3 films with (006)-dominant orientation. The cross-section image of CSP film (Fig. 3c) exhibited a uniform layer with smaller grains (60–600 nm) as compared to PVD layer. Hence, the density of grain boundaries (GBs) is higher in the CSP film. Considering a three-stage CISe deposition process, based on Cu-poor/Cu-rich/Cu-poor transition, a more defected In_2Se_3 film promotes higher grain sizes of the final layer through the reduction of density of defects (i.e. reduction of GBs) [31]. Thus, it could be expected that in a three-stage growth process involving the two CSP (first step) and PVD (second and third step) techniques, a higher density of GBs in the CSP-In_2Se_3 film results in effective grain growth of the final absorber layer.

The XPS results are shown in Fig. 6. Once again, the un-clean surface exhibited an O1s spectrum that consists of at least two sub-bands, one related to surface contamination (531.04 eV) and another oxygen bonded to metal (529.34 eV). After cleaning the surface, XPS shows peaks related to oxygen bonded to a metal [28]. From these results, it is possible to observe that the peak related to oxygen is higher in CSP films compared with PVD layers. Oxygen in the CSP film is likely replacing Se and thereby bonding to In to form In_2O_3. The presence of oxygen in the films can have different effects such as: i) passivation of surface dangling bonds related to Se vacancies (e.g. In_2O_3), and ii) formation of surface contamination (e.g. OH bonds). Barreau et al. [32] reported the disruption of crystallite growth of In_2S_3 thin films in the presence of OH bonds. The passivation of surface dangling bonds through the formation of In_2O_3 takes place on the interface states at the P–N junction of a solar cell or on grain boundaries in the bulk of the film. Passivation of GBs in the bulk is beneficial to the solar cell performance by reducing the number of recombination centers [33]. Passivation at the junction could be detrimental for the devices due to the enhanced interface recombination [34]. To avoid negative effects of oxygen passivation on the electrical properties of devices, the CSP-deposited In_2Se_3 precursor films could be subjected to different surface chemical treatments with NH_3 [35], HCl [36], etc, prior to the formation of CISe or CIGSe absorbers layers.

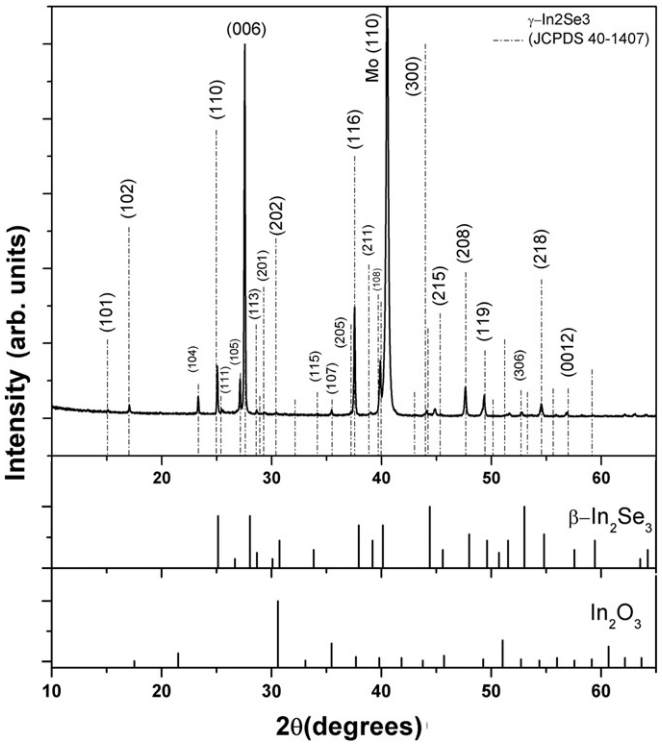

Fig. 5. XRD pattern of the In_2Se_3 film grown by CSP deposition.

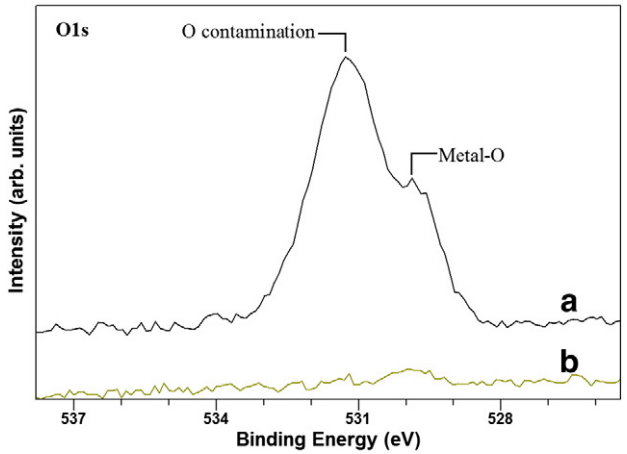

Fig. 4. XPS of the In_2Se_3 film grown by PVD, before (a) and after etching (b).

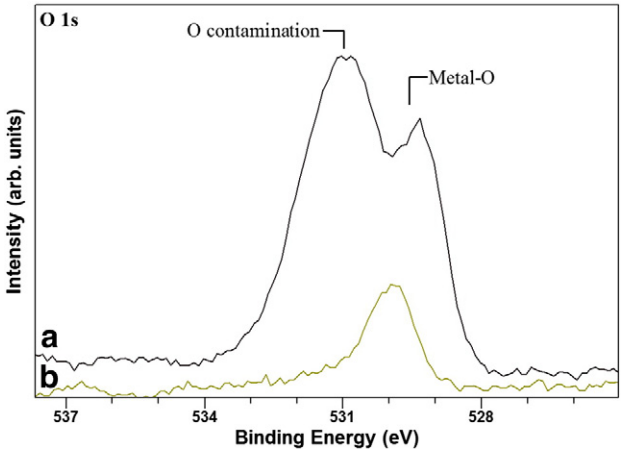

Fig. 6. XPS of the In_2Se_3 film grown by CSP, before (a) and after etching (b).

4. Conclusion

In this study, we showed that In_2Se_3 precursor thin films with similar structural properties and good uniformity could be deposited by CSP and PVD techniques. XRD and Raman spectroscopy showed that both films have same γ-In_2Se_3 crystalline phase. The PVD and CSP films exhibited a (110) and (006) preferred orientation, respectively. Both orientations, however, are related with CISe/CIGSe films with the same (112) preferential orientation. SEM images showed smaller grains in the CSP films compared to PVD layers. In a three-stage process involving the two CSP (first step) and PVD (second and third step) techniques, a higher number of GBs in the CSP-In_2Se_3 film could result in an effective grain growth of the final absorber layer. Another important characteristic that differentiates both precursor films is the oxygen contamination, which could be beneficial or detrimental to the electrical properties of the CISe based solar cell depending on its location. A chemical treatment of CSP In_2Se_3 films could be necessary in order to avoid detrimental effects of oxygen. Taking account of the obtained results, we suggest that the CSP films could be considered as precursor layer in a co-evaporation 3-stage process in order to produce CISe absorber films.

Acknowledgments

The authors would like to thank to the members of our research group in Université de Nantes (IMN) and Cinvestav-Zacatenco. This work is supported by the Consejo Nacional de Ciencia y Tecnología (grant 219494) and Université de Nantes (grant 219494). One of the authors (SV) wishes to thank the support from MSIP (Ministry of Science, Ict & future Planning) (141S-6-3-0641), South Korea.

References

[1] K.L. Chopra, P.D. Paulson, V. Dutta, Thin-films solar cells: an overview, Prog. Photovolt. 12 (2004) 69.
[2] L. Ying, K. Deyi, Preparation of Cu(In,Ga)Se_2 thin film by non-vacuum mechanochemical and spin coating, IEEE Asia-Pacific Power and Energy Engineering Conference, Wuhan, China, March 25–28, 2011.
[3] P. Jackson, D. Hariskos, R. Wuerz, W. Wischmann, M. Powalla, Compositional investigation of potassium doped Cu(In, Ga)Se2 solar cells with efficiencies up to 20.8%, Phys. Status Solidi (RRL) 8 (3) (2014) 219.
[4] M.A. Green, K. Emery, Y. Hishikawa, W. Warta, E.D. Dunlop, Prog. Photovolt. Res. Appl. 22 (2014) 1.
[5] I. Repins, M.A. Contreras, B. Egaas, C. DeHart, J. Scharf, C.L. Perkins, B. Noufi, 19.9 efficient ZnO/CdS/CIGS solar cells with 81.2% fill factor, Prog. Photovolt. Res. Appl. 16 (2008) 235.
[6] N. Barreau, J. Lahnemann, F. Couzinié-Devy, L. Assmann, P. Bertoncini, J. Kessler, Impact of Cu-rich growth on the $CuIn_{1-x}Ga_xSe_2$ surfae morphology and related solar cells behaviour, Sol. Energy Mater. Sol. Cells 93 (2009) 2013.
[7] K. Kushiya, T. Komaru, Y. Nakayama, T. Kume, Y. Suzuki, Technical Digest of 17th Photovoltaic Science and Engineering Conference, Fukuoka, Japan, December 3–7, 2007, p. 1796.
[8] M.E. Calixto, K.D. Dobson, B.E. McCandless, R.W. Birkmire, Growth mechanisms of electrodeposited $CuInSe_2$ and Cu(In,Ga)Se_2 determined by cyclic voltammetry, Materials Research Society Proceedings, Thin-Film Compound Semiconductor Photovoltaics Symposium, vol. 865, 2005, p. F14.17.1.
[9] M.G. Panthani, V. Akhavan, B. Goodfellow, J. Schmidtke, L. Dunn, A. Dodabalapur, P.F. Barbara, B.A. Korgel, Synthesis of CuInS, CuInSe and Cu(In, Ga)Se (CIGS) nanocrystal "inks" for printable photovoltaics, J. Am. Chem. Soc. 130 (49) (2008) 16770.
[10] D.L. Shulz, C.J. Curtis, A. Cram, J.L. Alleman, A. Mason, R.J. Matson, J.D. Perkins, D.S. Ginley, CIGS films via nanoparticle spray deposition: attempts at densifying a porous precursor, Conference Record of the 26th IEEE Photovoltaic Specialist Conference, California, USA, Sept–Oct 29–3, 1997, p. 483.
[11] B. Vidhya, S. Velumani, J.A. Arenas-Alatorre, A. Morales-Acevedo, R. Asomoza, J.A. Chavez-Carvayar, Structural studies of mechano-chemically synthesized $CuIn_{1-x}Ga_xSe_2$ nanoparticles, Mater. Sci. Eng. B 174 (2010) 216.
[12] B. Vidhya, S. Velumani, R. Asomoza, Effect of milling time and heat treatment on the composition of $CuIn_{0.75}Ga_{0.25}Se_2$ nanoparticles precursors and films, J. Nanoparticle Res. 13 (2011) 3033.
[13] C.R. Abernathy, C.W. Bates, A.A. Anani, B. Haba, G. Smestad, Production of single phase chalcopyrite $CuInSe_2$ by spray pyrolysis, Appl. Phys. Lett. 45 (2) (1984) 890.
[14] S. Duchemin, J. Bougnot, A. El Ghzizal, K. Belghit, Studies on the improvement of sprayed CdS–$CuInSe_2$ solar cells, Proceedings of the 9th European Photovoltaic Solar Energy Conference, Freiburg, September 25–29, 1989, p. 476.
[15] B.J. Babu, S. Velumani, R. Asomoza, An (ITO or AZO)/ZnO/Cu($In_{1-x}Ga_x$) Se_2 superstrate thin film solar cell structure prepared by spray pyrolysis, 37th IEEE Photovoltaic Specialist Conference, Washington, USA, June 19–24, 2011, p. 1238.
[16] B.J. Babu, S. Velumani, A. Morales-Acevedo, R. Asomoza, Properties of CuInGaSe thin films prepared by chemical spray pyrolysis, 7th International Conference on Electrical Engineering, Computing Science and Automatic Control, Chiapas, Mexico, September 8–10, 2010, p. 582.
[17] B.M. Basol, M. Pinarbasi, S. Aksu, J. Wang, Y. Matus, T. Johnson, Y. Matus, B. Metin, M. Narasimhan, D. Nayak, G. Norsworthy, D. Soltz, J. Wang, T. Wang, H. Zolla, Electroplating based technology for roll-to-roll manufacturing, 23rd European Photovoltaic Solar Energy Conference, Valencia, Spain, September 1–5, 2008, p. 2137.
[18] B.M. Basol, Low cost techniques for the preparation of Cu(In, Ga)(Se, S)2 absorber layers, Thin Solid Films 361–362 (2000) 514.
[19] J.B. Mooney, S.B. Radding, Spray pyrolysis processing, Annu. Rev. Mater. Sci. 12 (1982) 81.
[20] P. Jackson, D. Hariskos, E. Lotter, S. Paetel, R. Wuerz, R. Menner, W. Wischmann, M. Powalla, New world record efficiency for Cu(In, Ga)Se2 thin-film solar cells beyond 20%, Prog. Photovolt. 19 (2011) 894.
[21] S. Nishiwaki, T. Satoh, S. Hayashi, T. Negami, T. Wada, Preparation of Cu(In, Ga)Se2 thin films from In–Ga–Se precursors for high-efficiency solar cells, J. Mater. Res. 14 (12) (1999) 4514.
[22] T. Mise, T. Nakada, Microstructural properties of (In, Ga)2Se3 precursor layers for efficient CIGS thin-film solar cells, Sol. Energy Mater. Sol. Cells 93 (2009) 1000.
[23] A. Likforman, D. Carre, R. Hillel, Structure crystalline du seleniure d'indium In_2Se_3, Acta Crystallogr. B 34 (1978) 1.
[24] K. Kambas, C. Julien, M. Jouanne, A. Likforman, M. Guittard, Raman spectra of alpha α- and γ-In_2Se_3, Phys. Status Solidi B 124 (1984) K105.
[25] R. Lewandowska, R. Bacewicz, J. Filipowicz, W. Paszkowicz, Raman scattering in α-In_2Se_3 crystals, Mater. Res. Bull. 36 (2001) 2577.
[26] I. Watanabe, T. Yamamoto, Electrical and structural properties of amorphous In–Se films prepared by flash evaporation, Jpn. J. Appl. Phys. 24 (1985) 1282.
[27] S. Marsillac, A.M. Combat-Marie, J.C. Bernede, A. Conan, Experimental evidence of the low-temperature formation of γ-In_2Se_3 thin films obtained by solid-state reaction, Thin Solid Films 288 (1996) 14.
[28] J.F. Moulder, C.D. Wagner, W.M. Riggs, L.E. Davis, Handbook of X-ray Photoelectron Spectroscopy, Perkin-Elmer Corporation, Minnesota, 1979.
[29] J.C. Viguié, J. Spitz, Chemical vapor deposition at low temperatures, J. Electrochem. Soc.: Solid-State Technol 122 (4) (1975) 585.
[30] S. Ishizuka, A. Yamada, P. Fons, S. Niki, Texture and morphology variation in (In, Ga)2Se3and Cu(In, Ga)Se2 thin films grown with various Se source conditions, Prog. Photovolt. Res. Appl. 21 (2011) 544.
[31] N. Barreau, T. Painchaud, F. Couzinié-Devy, L. Arzel, J. Kessler, Recrystallization of CIGSe layers grown by three-step process: a model based on grain boundary migration, Acta Mater. 58 (2010) 5572.
[32] N. Barreau, J.C. Bernède, H. El Maliki, S. Marsillac, X. Castel, J. Pinel, Recent studies on In_2S_3 containing oxygen thin films, Solid State Commun. 122 (2002) 445.
[33] D. Cahen, R. Noufi, Defect chemical explanation for the effect of air anneal on CdS/$CuInSe_2$ solar cell performance, Appl. Phys. Lett. 54 (1989) 558.
[34] L. Kronik, D. Cahen, Effects of sodium on polycrystalline Cu(In, Ga)Se2 and its solar cell performance, Adv. Mater. 10 (1998) 31.
[35] R. Hunger, T. Schulmeyer, A. Klein, W. Jaegermann, M.V. Lebedev, K. Sakurai, S. Niki, SXPS investigation of the Cd partial electrolyte treatment of $CuInSe_2$ absorbers, Thin Solid Films 480–481 (2005) 218.
[36] H. Maki, T. Ikoma, I. Sakaguchi, N. Ohashi, H. Haneda, J. Tanaka, N. Ichinose, Control of surface morphology of ZNO (000-1) by hydrochloric acid etching, Thin Solid Films 411 (2002) 91.